



Structurally characterized homotrinary Salamo-type nickel(II) complexes: Synthesis, solvent effect and fluorescence properties

Quan-Peng Kang | Xiao-Yan Li | Qing Zhao | Jian-Chun Ma | Wen-Kui Dong

School of Chemical and Biological Engineering, Lanzhou Jiaotong University, Lanzhou 730070, P. R. China

Correspondence

Wen-Kui Dong, School of Chemical and Biological Engineering, Lanzhou Jiaotong University, Lanzhou 730070, China. Email: dongwk@126.com

Funding information

National Natural Science Foundation of China, Grant/Award Number: 21761018; Program for Excellent Team of Scientific Research in Lanzhou Jiaotong University, Grant/Award Number: 201706

Four new solvent-induced Ni(II) complexes with chemical formulae $[\{\text{NiL}(\mu_2\text{-OAc})(\text{MeOH})\}_2\text{Ni}] \cdot 2\text{MeOH}$ (**1**), $[\{\text{NiL}(\mu_2\text{-OAc})\}_2(\text{n-PrOH})(\text{H}_2\text{O})\text{Ni}] \cdot \text{n-PrOH}$ (**2**), $[\{\text{NiL}(\mu_2\text{-OAc})(\text{DMF})\}_2\text{Ni}]$ (**3**) and $[\{\text{NiL}(\mu_2\text{-OAc})(\text{DMSO})\}_2\text{Ni}] \cdot 2\text{DMSO}$ (**4**), ($\text{H}_2\text{L} = 4\text{-Nitro-4'-chloro-2,2'-(1,3-propylene)dioxybis(nitrilomethylidyne)}$) diphenol) have been synthesized and characterized by elemental analyses, FT-IR, UV-Vis spectra and X-ray crystallography. X-ray crystal structure determinations revealed that each of the Ni(II) complexes **1–4** consists of three Ni(II) atoms, two completely deprotonated (L^{2-}) units, two μ_2 -acetate ions and two coordinated solvent molecules (solvents are methanol, n-propanol, water, N, N-dimethylformamide and dimethyl sulphoxide, respectively). Although the four complexes **1–4** were synthesized in different solvents, it is worthwhile that the Ni(II) atoms in the four complexes **1–4** adopt hexa-coordinated with slightly distorted octahedral coordination geometries, and the ratios of the ligand H_2L to Ni(II) atoms are all 2: 3. The complexes **1–4** possess self-assembled infinite 1D, 3D, 1D and 2D supramolecular structures via the intermolecular hydrogen bonds, respectively. In addition, fluorescence behaviors were investigated in the complexes **1–4**.

KEYWORDS

fluorescence property, salamo-type Ni(II) complex, solvent effect, structure, synthesis

1 | INTRODUCTION

Salen-like complexes have been extensively investigated in the past decades since the synthesis of Salen (*N, N'*-bis(salicylaldehyde)ethylenediamine) was first reported.^[1–5] Moreover, the potential catalytic behavior of the Salen-type species, especially in the areas of asymmetric catalysis,^[6,7] was gradually recognized on the basis of wide research works. The transition metal complexes with Salen-type ligands have excellent properties, such as biological fields,^[8–14] unusual magnetic^[15–17] and electrochemical behaviors,^[18] supramolecular architectures,^[19–23] molecular recognitions^[24–27]

and luminescence properties.^[28–32] It is significant to introduce appropriate functional groups into the organic parts of the ligands to regulate the characteristics of these metal complexes.^[33–36] With respect to these complexes, phenoxo bridging plays an important role in assembling metal ions and Salen-type ligands. There are also reports of changes in the length of methylene chains of Salen complexes, which includes trialkylene, tetraalkylene, or longer alkylene chains.^[37] The chain length of methylene of the Salen-type complex will lead to different coordination environment of the central metal ions.

Recently, Salamo-type ligand as a novel Salen-type analogue has been studied in modern coordination

chemistry and organometallic chemistry. Salamo-type ligand ($R-CH=N-O-(CH_2)_n-O-N=CH-R$) is one of the most versatile ligands. It is expected that the large electronegativity of oxygen atoms will strongly influence the electronic properties of the N_2O_2 coordination sphere, leading to different structures and characteristics of the complexes. Owing to the special structures of Salamo-type complexes, a study was shown that it is at least 104 times more stable than Salen-type complexes.^[38] Herein, we report the syntheses, crystal structures and solvent effects of four homotrimeric complexes, $[[NiL(\mu_2-OAc)(MeOH)]_2Ni] \cdot 2MeOH$ (**1**), $[[NiL(\mu_2-OAc)]_2(n-PrOH)(H_2O)Ni] \cdot n-PrOH$ (**2**), $[[NiL(\mu_2-OAc)(DMF)]_2Ni]$ (**3**) and $[[NiL(\mu_2-OAc)(DMSO)]_2Ni] \cdot 2DMSO$ (**4**), the complexes **1–4** were characterized by elemental analyses, IR, UV-Vis spectra and X-ray single crystallography.

2 | RESULTS AND DISCUSSION

2.1 | IR spectra analyses

IR spectra of H_2L and its corresponding Ni(II) complexes **1–4** exhibited various bands in the region of $400-4000\text{ cm}^{-1}$ region (Figure 1). It is obvious that the typical $\nu(O-H)$ absorption band was near 3084 cm^{-1} in the spectrum of H_2L . A typical $C=N$ stretching band of the free ligand H_2L appeared at 1605 cm^{-1} , and those of complexes **1–4** appeared at 1606 , 1608 , 1606 and 1613 cm^{-1} , respectively.^[39,40] The $C=N$ stretching frequencies are shifted to high frequencies, indicating that the Ni(II) atoms are coordinated by oxime nitrogen atoms of deprotonated $(L)^{2-}$ moieties. Therefore, conclusion could be made that the ligand H_2L has coordinated with Ni(II) atoms.^[41,42] The typical $Ar-O$ stretching frequency is a strong band at $1231-1263\text{ cm}^{-1}$, which is similar to previously

reported Salen-type ligands.^[43] Meanwhile, the free ligand H_2L exhibited a typical $Ar-O$ stretching frequency at 1263 cm^{-1} , while those of complexes **1–4** appeared at 1256 , 1253 , 1250 and 1250 cm^{-1} , respectively. The $Ar-O$ stretching frequencies are shifted to lower frequencies, indicating that Ni–O bonds are formed between the Ni(II) atoms and oxygen atoms of phenolic groups.^[44]

The far-infrared spectra of the Ni(II) complexes **1–4** were obtained from $100-550\text{ cm}^{-1}$ to identify frequencies due to the Ni–O and Ni–N bonds. The bands appeared at 513 , 519 , 519 and 525 cm^{-1} in the Ni(II) complexes **1–4** could be attributed to $\nu(Ni-N)$, while the bands appeared at 474 , 487 , 474 and 468 cm^{-1} were assigned to $\nu(Ni-O)$, which is in consistent with the literature frequency values.^[45,46]

2.2 | UV-vis absorption spectra

UV-vis absorption spectra of H_2L and its corresponding complexes **1–4** were determined in $1.0 \times 10^{-5}\text{ M}$ ethanol solution, as shown in Figure 2. Absorption spectra of the complexes **1–4** showed that the complexes **1–4** have similar absorption spectra, but are different from the spectrum of H_2L . UV-vis spectrum of H_2L exhibited three absorptions at *ca.* 219, 267 and 311 nm. The absorptions at 219 and 267 nm can be assigned to $\pi-\pi^*$ transitions of the benzene rings, while the absorption at 311 nm can be attributed to intraligand $\pi-\pi^*$ transitions of $C=N$ groups.^[47–49] Compared with the absorption peak of the free ligand, the corresponding absorption peaks of the complexes **1–4** are bathochromically shifted and were observed at *ca.* 230–233 nm, indicating the phenolic oxygen and oxime nitrogen atoms are involved in coordination to the Ni(II) atoms. The absorption peaks at *ca.* 267 and 311 nm were absent in the complexes **1–4**.

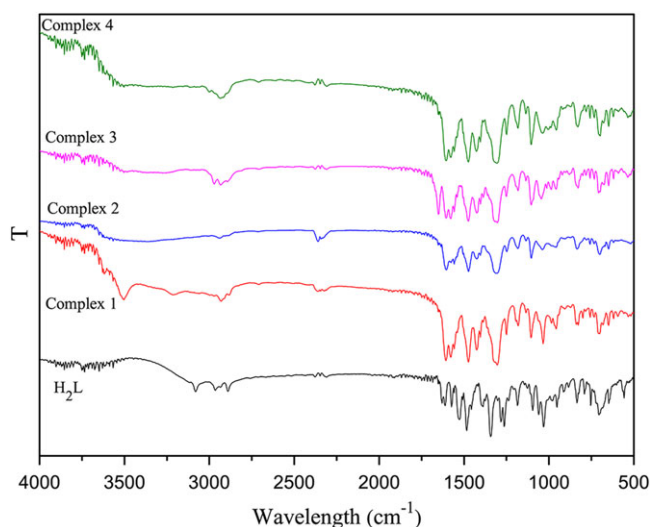


FIGURE 1 Infrared spectra of H_2L and its complexes **1–4**

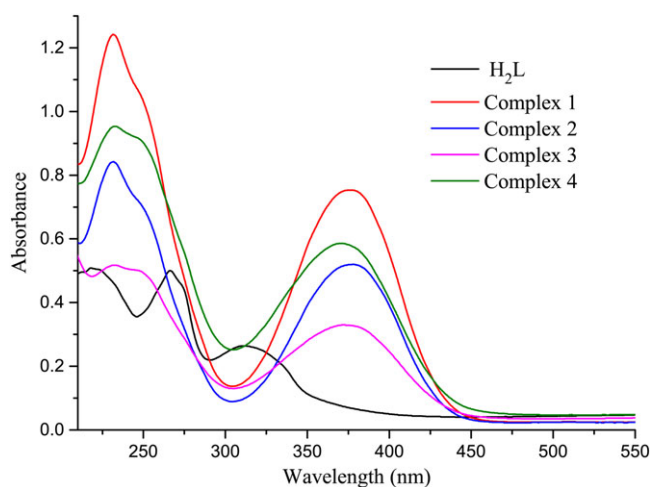


FIGURE 2 UV-vis spectra of H_2L and its complexes **1–4** in ethanol ($c = 1.0 \times 10^{-5}\text{ M}$)

Meanwhile, new absorption peaks were observed at *ca.* 370–376 nm in the complexes **1–4**, may be due to $L \rightarrow M$ charge-transfer transitions, which are characteristic of the transition metal complexes with Salen-type N_2O_2 coordination spheres.

2.3 | Descriptions of the crystal structures

Selected bond lengths (Å) and angles (°) are presented in Table S1. Hydrogen bonds in the Ni(II) complexes **1–4** are given in Table S2.

2.3.1 | Crystal structures of the Ni(II) complexes **1** and **4**

The X-ray crystal structure analyses of the complexes **1** and **4** revealed that they have the similar symmetrical trinuclear molecular unit $[\{NiL(\mu_2-OAc)(solvent)\}_2Ni] \cdot 2solvent$ (the solvents are MeOH and DMSO in the complexes **1** and **4**, respectively), as shown in Figures 3 and 4, respectively. While the different solvents observed lead to the formation of the typical solvent-induced the Ni(II) complexes.^[50]

The crystal structure of the Ni(II) complex **1** is shown in Figure 3. The complex **1** crystallizes in the triclinic system, space group $P\bar{1}$ with $Z = 1$. The molecular structure of complex **1** consists of three Ni(II) atoms, two completely deprotonated $(L)^{2-}$ units, two μ_2 -acetate ions, two coordinated methanol molecules and two non-coordinated methanol molecules resulting in a trinuclear Ni(II) complex. The terminal Ni(II) atom (Ni2 or Ni2^{#1}) is hexa-coordinated by two oxime nitrogen (N1 and N2) and two phenolic oxygen (O3 and O4) atoms of the deprotonated Salamo-type $(L)^{2-}$ unit, one oxygen atom (O5) from the coordinated μ_2 -acetate ion and the other oxygen atom (O7) from the coordinated methanol molecule. The dihedral angle between the coordination planes of N1–Ni2–O3 and N2–Ni2–O4 is 7.80(2)°, indicating the coordination geometry around the terminal Ni(II) atom is a slightly distorted octahedron.

However, the coordination sphere of the central Ni(II) (Ni1) atom is completed by four phenoxo oxygen (O3, O4, O3^{#1} and O4^{#1}) atoms from two deprotonated $(L)^{2-}$ moieties and two μ_2 -acetato oxygen (O6 and O6^{#1}) atoms. Ni1 is bridged by Ni2 and Ni2^{#1} through two bridging μ_2 -acetate ions in a similar $\mu-O-C-O$ fashion.^[51,52] As a result the central Ni1 atom finally has an $O_2O_2O_2$ coordination environment. Then all of the hexa-coordinated Ni(II) atoms of the complex **1** have slightly distorted octahedral geometries. The crystal structure of the complex **4** is very similar to that of the complex **1** (Figure 4).

The intramolecular and intermolecular hydrogen bonding interactions of the complex **1** are given in

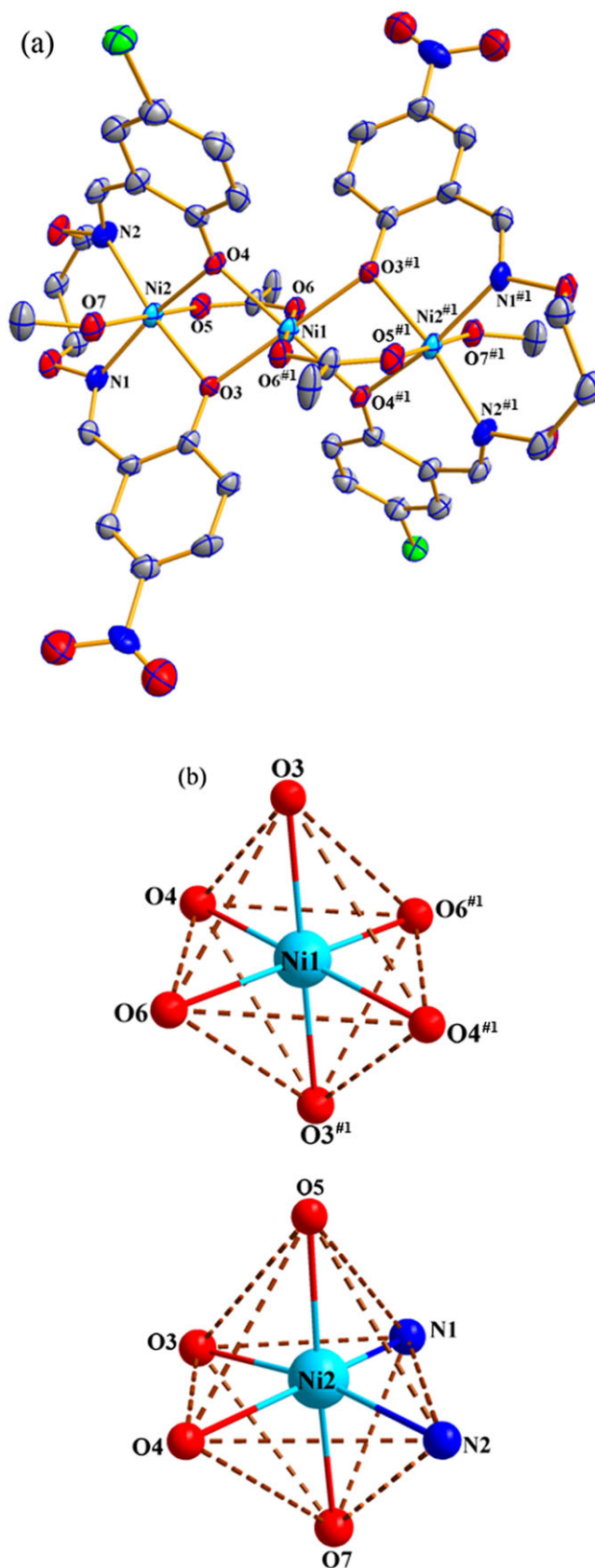


FIGURE 3 (a) Molecular structure and atom numberings of the complex **1** with 30% probability displacement ellipsoids (hydrogen atoms are omitted for clarity); (b) Coordination polyhedrons for Ni(II) atoms of the complex **1**

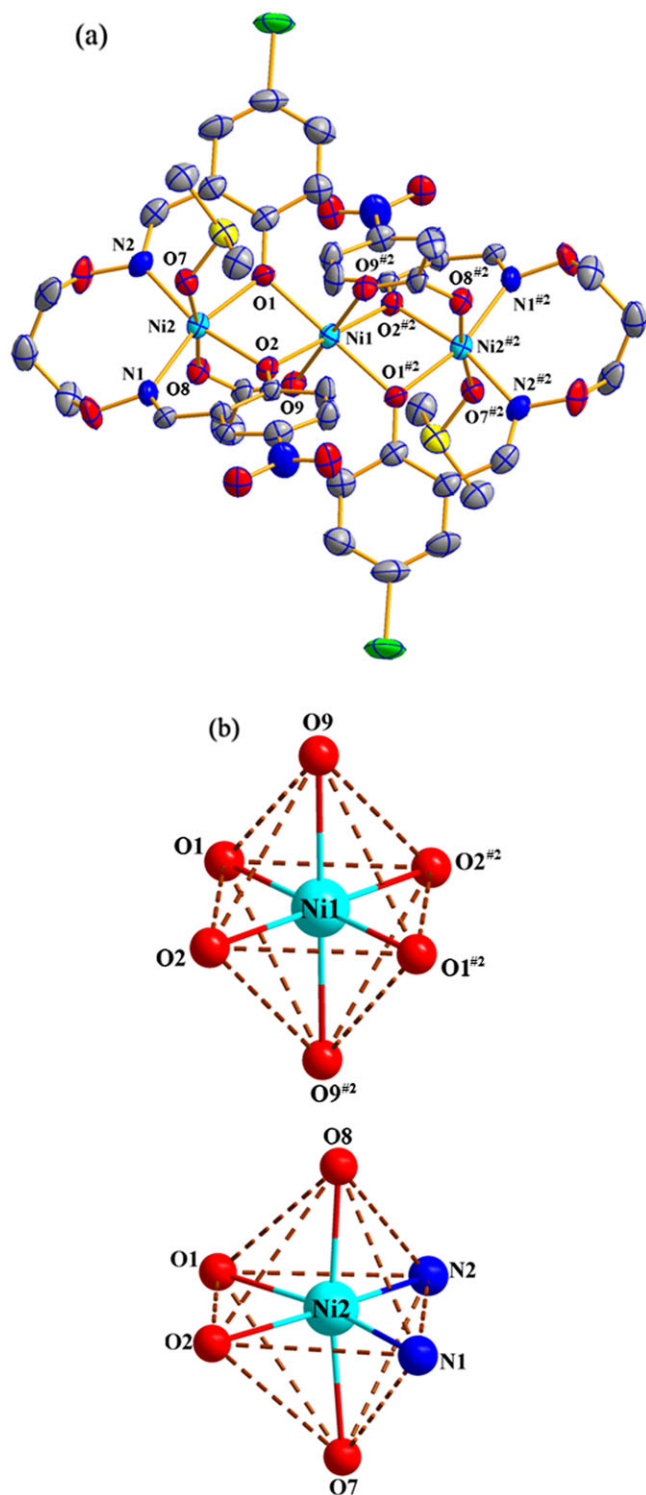


FIGURE 4 (a) Molecular structure and atom numberings of the complex 4 with 30% probability displacement ellipsoids (hydrogen atoms are omitted for clarity); (b) Coordination polyhedrons for Ni(II) atoms of the complex 4

Figures 5 and 6, and those of the complex 4 are given in Figures 7 and 8, respectively. In the crystal structures of the complexes 1 and 4, the structures are connected by three and four pairs of intramolecular hydrogen bonding

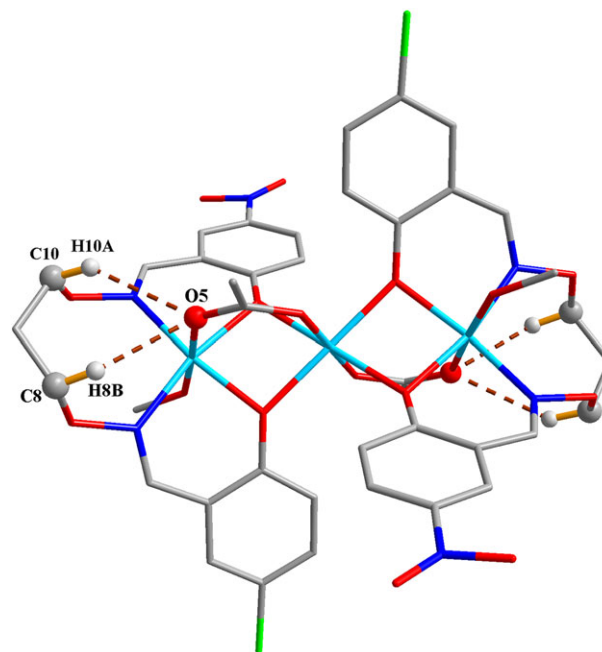


FIGURE 5 View of the intramolecular hydrogen bonds of the complex 1

interactions, respectively, which plays a vital role in constructing and stabilizing the complexes 1 and 4 molecules. As shown in the Figures 6 and 8, the neighboring complex molecules are further linked into an infinite 1D and 2D supramolecular structure by three and a pairs of intermolecular hydrogen bonds, respectively. (In complex 1: O7–H7A...O10, C O10–H10...O6, C19–H19B...O9; in complex 4: C8–H8A...O5A) (Table S2).^[53–56]

2.3.2 | Crystal structure of the Ni(II) complex 2

The X-ray crystallographic analysis of the complex 2 revealed an asymmetric trinuclear structure. It crystallizes in the orthorhombic system, space group $P2_12_12_1$ with $Z = 4$. The molecule consists of three Ni(II) atoms, two completely deprotonated (L)²⁻ units, two μ_2 -acetate ions, one coordinated n-propanol molecule, one crystallizing water molecule and one non-coordinated n-propanol molecule.

As shown in Figure 9. Two terminal Ni(II) atom (Ni1 or Ni3) is located at the N_2O_2 coordination spheres of Salamo moieties, while the third one (Ni2) is located in the central cavity. The three Ni(II) atoms were bridged by the two μ_2 -acetate groups. Two terminal Ni(II) (Ni1 or Ni3) atom is hexa-coordinated by two oxime nitrogen (N1, N2 or N4, N5) atoms, two deprotonated phenoxo-oxygen (O1, O4 or O7, O10) atoms of the (L)²⁻ units, one oxygen (O13 or O15) atom of one μ_2 -acetate ion, and other oxygen (O19 or O17) atom comes from the coordinated water or n-propanol molecule that the axial

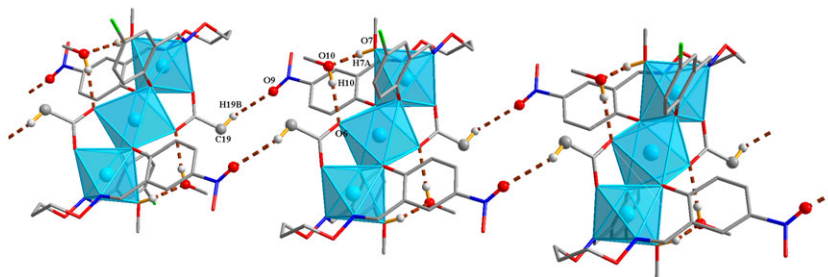


FIGURE 6 Part of the infinite 1D supramolecular chain of the complex **1**

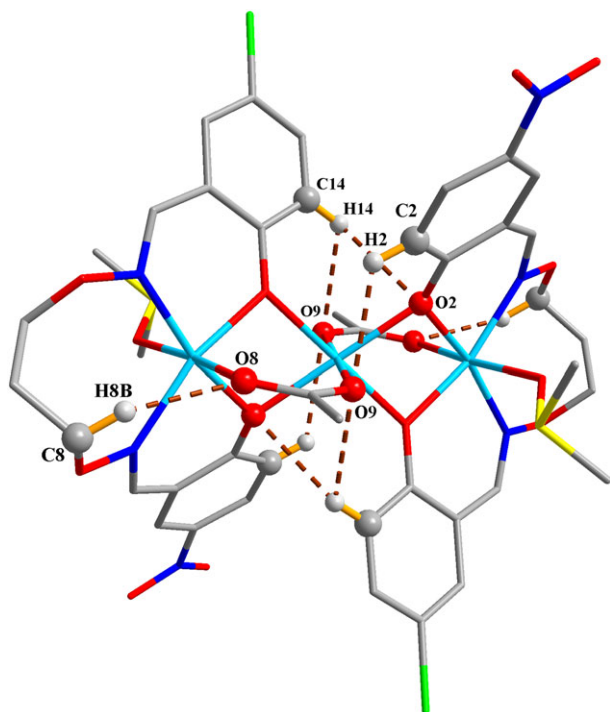


FIGURE 7 View of the intramolecular hydrogen bonds of the complex **4**

positions. The dihedral angle between coordination planes of N1–Ni1–O1 and N2–Ni1–O4 is $7.73(5)^\circ$. The dihedral angle between coordination planes of N4–Ni3–O7 and N5–Ni3–O10 is $7.94(2)^\circ$. These indicate that the Ni(II) (Ni1 or Ni3) atom forms a slightly distorted octahedral geometry. The primary Ni–N and Ni–O distances are in the normal ranges (Ni1–N1 = 2.054(9), Ni1–N2 = 2.052(11), Ni1–O1 = 2.036(7), Ni2–O4 = 2.034(8), Ni2–O19 = 2.108(2) and Ni2–O13 = 2.007(2) Å) (Table S1). The bond length between the Ni(II) atom and the apical oxygen (O19) atom is 2.108(2) Å, which is obviously longer than the distances between the Ni(II) atom and the basal oxygen and nitrogen atoms. This significant elongation has been observed previously in the Ni(II) complexes with Salamo-type ligands. The Ni3 atom is similar to Ni1 atom.

In addition, the central Ni(II) (Ni2) atom is also located in a hexa-coordinated environment, The coordination sphere of the central Ni(II) atom (Ni2) contains

four phenoxo oxygen (O1, O4, O7 and O10) atoms from two deprotonated (L)²⁻ units and double μ_2 -acetate oxygen (O14 and O16) atoms that adopt a similar μ -O–C–O fashion. As a result the central Ni2 atom finally has an O₂O₂O₂ coordination environment. The primary Ni–O distances are in the normal ranges (Ni2–O1 = 2.062(7), Ni2–O4 = 2.078(8), Ni2–O7 = 2.083(7), Ni2–O10 = 2.086(8), Ni2–O14 = 1.993(8) and Ni2–O16 = 2.071(8) Å) (Table S1).

As depicted in Figure 10, in the complex **2**, eleven pairs of intramolecular hydrogen bonds are formed, which plays a vital role in constructing and stabilizing the complex **2** molecules.^[53–56] The complex **2** is further linked by intermolecular hydrogen bonding interactions form a 3D supramolecular structure (Figure 11).

2.3.3 | Crystal structure of the Ni(II) complex **3**

The results of the X-ray structural study revealed that the complex **3** crystallizes in the triclinic system and *P*-1 space group. As depicted in Figure 12. The molecular structure of complex **3** consists of three Ni(II) atoms, two completely deprotonated (L)²⁻ units, two μ_2 -acetate ions and two coordinated DMF molecules.

The terminal Ni(II) (Ni2 or Ni2^{#3}) atom is hexa-coordinated by two oxime nitrogen (N1, N2 or N1^{#3}, N2^{#3}) atoms and two phenoxo oxygen (O1, O4 or O1^{#3}, O4^{#3}) atoms, the four atoms are all from one deprotonated (L)²⁻ units, one oxygen (O8 or O8^{#3}) atom from the μ_2 -acetate ions and one oxygen (O9 or O9^{#3}) atom from the coordinated DMF molecules. The central Ni(II) (Ni1) atom is also hexa-coordinated via four phenoxo oxygen atoms from two (L)²⁻ units, and two oxygen (O7 or O7^{#3}) atoms from μ_2 -acetate ions, The Ni1 and Ni2 (or Ni1 and Ni2^{#3}) atoms are connected through μ_2 -acetate ions in a familiar μ -O–C–O fashion. The coordination environment around all the Ni(II) atoms are best described as slightly distorted octahedral geometries.

As depicted in Figure 13, in the complex **3**, there are eight pairs of intramolecular (C2–H2...O7, C8–H8B...O3, C10–H10B...O2, C10–H10B...O8, C16–H16...O1, C16–H16...O7, C20–H20...O7 and C22–H22B...O9) hydrogen bonds are formed, which performs a crucial role in

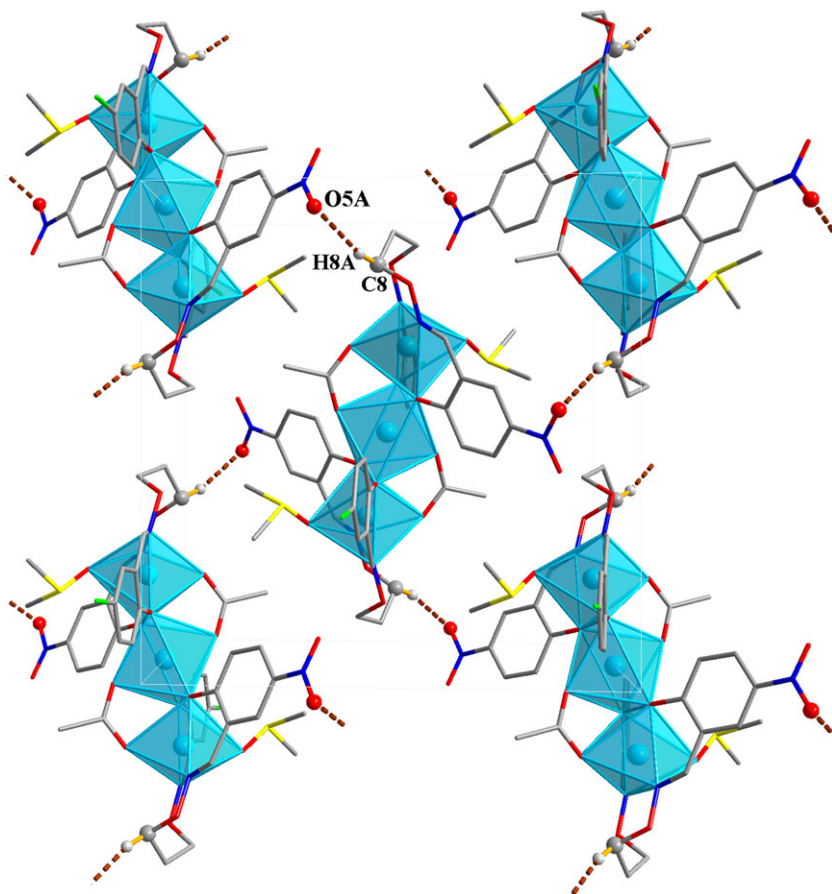


FIGURE 8 Part of the infinite 2D supramolecular network of the complex **4**

constructing and stabilizing supramolecular structure. Furthermore, every molecule links other molecules via intermolecular hydrogen bonds (C21–H21C...O5A) forming a 1D supramolecular structure (Table S2) (Figure 14).^[53–56]

To sum up, here we reported four homotrimeric Salamo-type Ni(II) complexes. In previous reports, the Salamo-type Ni(II) complexes are essentially mono-,^[57,58] di-,^[29] tri-,^[43] and hepta-nuclear,^[59] and the ratios of the ligand to Ni atoms are 1:1, 2:2, 2:3 and 2:7. Here we have successfully designed and synthesized a different ligand by changing the synthetic routes of Salamo-type ligands, including introducing asymmetric aldehydes or changing the length of methylene chains. The corresponding complexes were synthesized by the introduction of different solvents, in order to further promote the study of its structure and properties.

2.4 | Solvent effect

The four Ni(II) complexes could be synthesized by the reaction of the Salamo-type ligand H₂L with Ni(OAc)₂·4H₂O in different solvents. The complexes **1–4** presented similar stoichiometry ratio and molecular structures when different solvent molecules were

introduced. However, they possessed different supramolecular structure characteristics. The Ni(II) complexes **1–4** self-assemble into infinite 1D, 3D, 1D and 2D supramolecular structures through intermolecular hydrogen bonding interactions, respectively. In the Ni(II) complexes **1–4**, the solvent effect clearly showed the changes in bond distances (Å) and angles (°) (Table S1). It is noteworthy that the bond lengths from the oxygen (O7 and O17) atoms of the coordinated solvent molecules (methanol or n-propanol) to the terminal Ni(II) atoms in the Ni(II) complexes **1** and **2** are 2.112(5) and 2.161(8) Å, respectively, due to larger steric hindrance of the n-propanol than the methanol. Thus, solvent effects could explain their slight differences in crystal structures.

Experiments show that the methanol, n-propanol and acetone solution systems are suitable for the growth of complexes **1–4** single crystals, about two weeks later the single-crystal obtained can be used to analysis. When only methanol and acetone solution system, the methanol molecules can coordinate to the two terminal Ni(II) atoms in the axial position, while DMF or DMSO molecule can replace methanol and coordinate to the axial positions of the two terminal Ni(II) atoms when DMF or DMSO molecule is added into the system. In the n-propanol and acetone solution systems, water was added and it

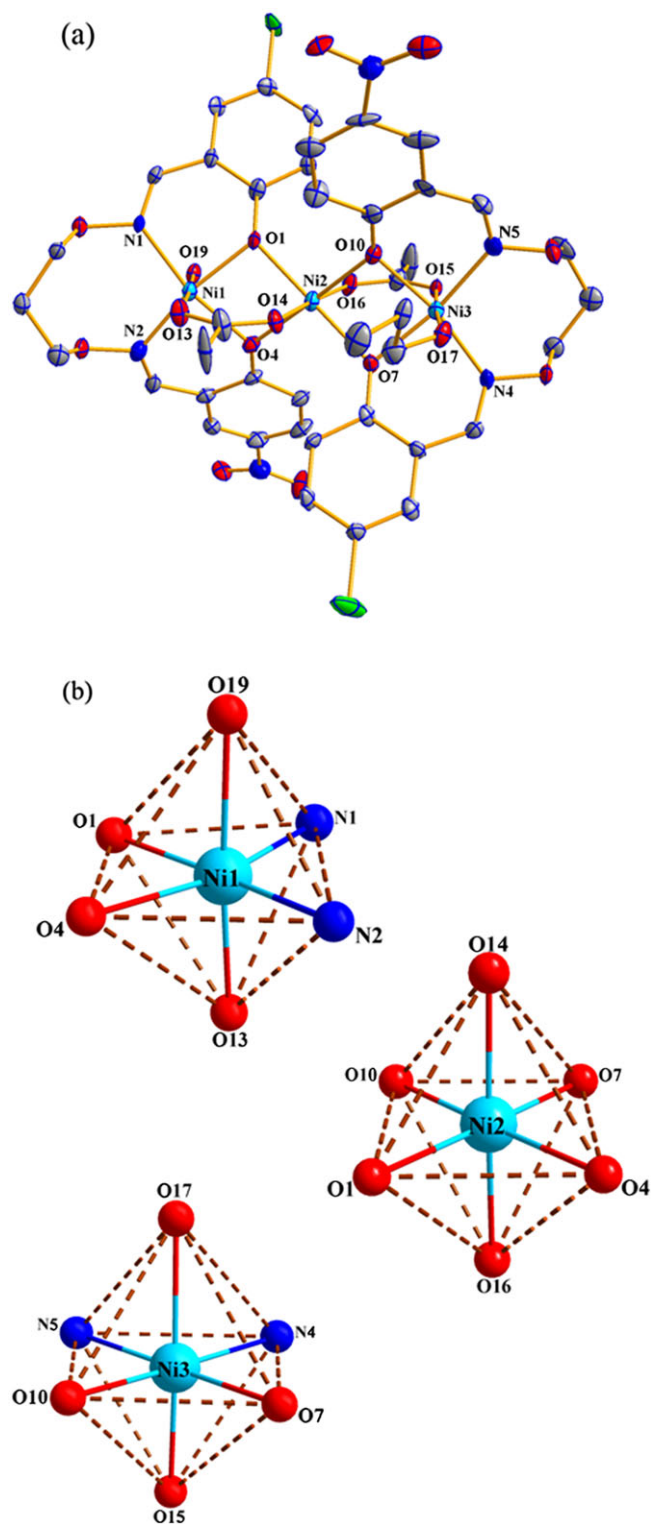


FIGURE 9 (a) Molecular structure and atom numberings of the complex 2 with 30% probability displacement ellipsoids (hydrogen atoms are omitted for clarity); (b) Coordination polyhedrons for Ni(II) atoms of the complex 2

was found that n-propanol and water molecules are involved in the coordination of two terminal Ni(II) atoms. A series of reaction processes show that the coordination ability of DMF or DMSO > methanol, n-propanol \approx water.

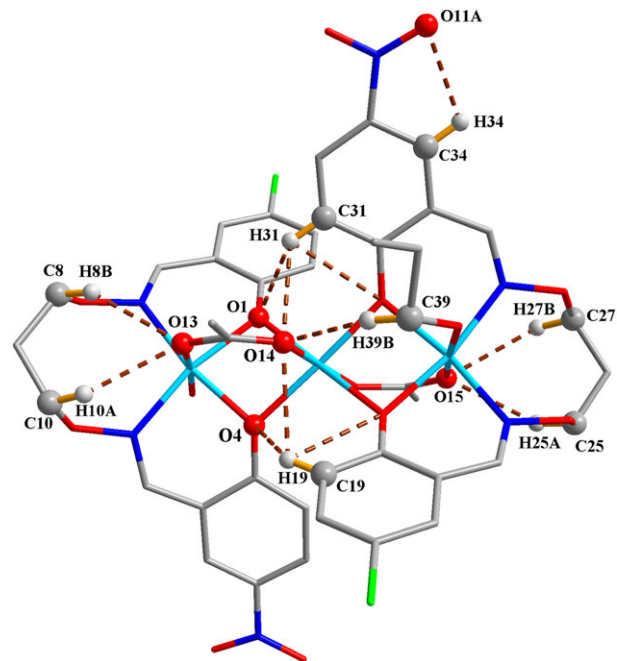


FIGURE 10 View of the intramolecular hydrogen bonds of the complex 2

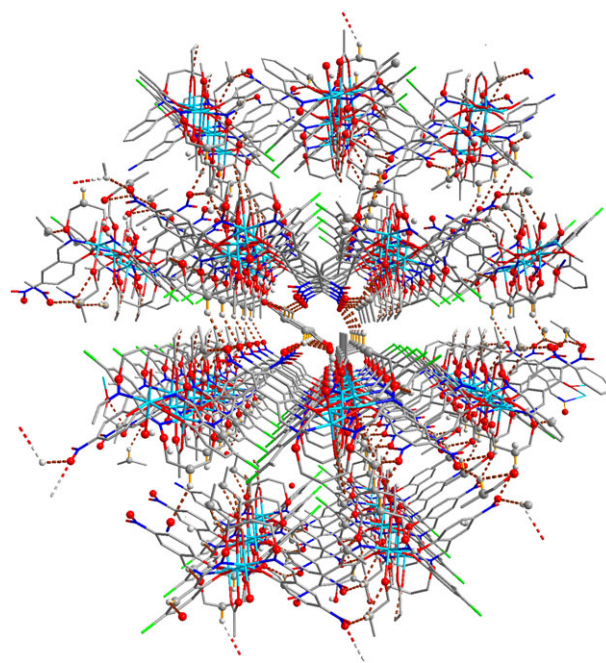


FIGURE 11 Part of the infinite 3D supramolecular structure showing the hydrogen bonding interactions of the complex 2

2.5 | Fluorescence properties

The fluorescence properties of H₂L and its corresponding complexes 1–4 were investigated at room temperature (Figure 15). The ligand H₂L exhibited an intense emission peak at 472 nm upon excitation at 365 nm, which should

significantly, indicating that the Ni(II) ions have the properties of fluorescent quenching.

3 | CONCLUSIONS

In summary, as a result of the introduction of different solvent molecules, four new homotrimeric Ni(II) complexes **1–4** with an asymmetric Salamo-type N_2O_2 ligand, were successfully designed and synthesized. X-ray crystal structure analyses of the Ni(II) complexes revealed that the structures of the Ni(II) complexes **1–4** are basically similar to each other. The Ni(II) complexes **1–4** differ only by the solvent molecules coordinated to central Ni(II) ions. Two terminal Ni(II) ions are located at the N_2O_2 coordination spheres of Salamo moieties, The terminal Ni(II) and central Ni(II) atoms are connected through μ_2 -acetate ions in a familiar μ -O-C-O fashion. All the hexa-coordinated Ni(II) atoms of the Ni(II) complexes **1–4** have slightly distorted octahedral coordination polyhedrons. Significantly, these Ni(II) complexes possess basically similar structures, but the supramolecular structures are entirely different. The Ni(II) complexes **1–4** possess self-assembling infinite 1D, 3D, 1D and 2D supramolecular structures via the intermolecular hydrogen bonds, respectively. The fluorescent spectra exhibited that the complexes **1–4** have weak fluorescent emissions.

4 | EXPERIMENTAL SECTION

4.1 | Materials and methods

5-Chlorosalicylaldehyde and 5-nitrosalicylaldehyde of 98% purity have been used without further purification. 1,3-Dibromopropane and other reagents were analytical grade reagents from Tianjin Chemical Reagent Factory.

Carbon, hydrogen and nitrogen analyses were obtained using a GmbH VarioEL V3.00 automatic elemental analysis instrument. Elemental analyses for Ni(II) were carried out by an IRIS ER/SWP-1 ICP atomic emission spectrometer. Melting points were measured by the use of a microscopic melting point apparatus made by Beijing Taike Instrument Limited Company. IR spectra were recorded on a VERTEX70 FT-IR spectrophotometer, with samples prepared as KBr ($400\text{--}4000\text{ cm}^{-1}$) pellets. UV-Vis absorption spectra were recorded on a Hitachi U-3900H spectrometer. ^1H NMR spectra were determined by German Bruker AVANCE DRX-400 spectrometer. X-ray single crystal structure determinations for the complexes **1–4** were carried out on a Bruker Smart Apex CCD (complex **1**) or SuperNova Dual Eos (Cu at zero)

four-circle (complexes **2–4**) diffractometer. Fluorescence spectra were carried out on F-7000 FL spectrophotometer.

4.2 | Crystal structure determinations of the complexes 1–4

The crystal and structure refinement data for the complexes **1–4** are given in Table 1. The single crystals of the Ni(II) complexes **1–4** with approximate dimensions of $0.18 \times 0.15 \times 0.11$, $0.13 \times 0.11 \times 0.04$, $0.31 \times 0.26 \times 0.25$ and $0.31 \times 0.25 \times 0.24$ mm were placed on a SuperNova, Dual (Cu at zero) Eos. diffractometer or Bruker Smart diffractometer equipped with Apex CCD area detector, respectively. The diffraction data were collected using a graphite monochromated Mo $K\alpha$ radiation ($\lambda = 0.71073\text{ \AA}$) at 296(2), 150.00(10), 294(2) and 294.54(10) K, respectively. The structures were solved by using the program SHELXS-2014^[62] and Fourier difference techniques, and refined by full-matrix least-squares method on F^2 with SHELXL-2014.^[63] Anisotropic thermal parameters were used for the nonhydrogen atoms and isotropic parameters for the hydrogen atoms. Hydrogen atoms were added geometrically and refined using a riding model.

4.3 | Synthesis and characterization of H_2L

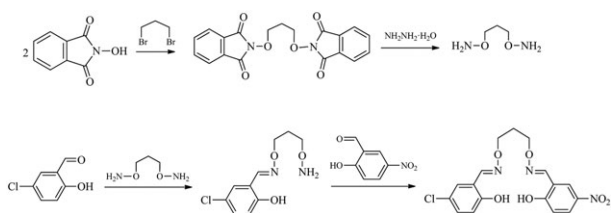
The main reaction steps involved in the synthesis of H_2L is given in Scheme 1. 1,3-Bis(aminoxy)propane was synthesized according to an analogous method reported earlier.^[64]

The Salamo-type N_2O_2 ligand H_2L was synthesized according to an analogous method reported earlier.^[38,65] To an ethanol solution (80 ml) of 5-chlorosalicylaldehyde (626.0 mg, 4.0 mmol) was added an ethanol solution (50 ml) of 1,3-bis(aminoxy)propane (637.0 mg, 6.0 mmol). The mixture solution was heated at $50\text{--}55\text{ }^\circ\text{C}$ for 6 h. The solution was concentrated in *vacuo* and the residue was purified by column chromatography (SiO_2 , chloroform/ethyl acetate, 10:1) to afford colorless flocculent crystalline solid of 2-[O-(1-ethoxyamide)]oxime-4-chlorophenol (655.0 mg, 2.68 mmol). Yield, 66.9%. Anal. calc. For $C_{10}H_{13}ClN_2O_3$ (%): C, 49.09; H, 5.36; N, 11.45. Found (%): C, 49.31; H, 5.47; N, 11.22.

A solution of 2-[O-(1-ethoxyamide)]oxime-4-chlorophenol (489 mg, 2.0 mmol) in ethanol (15 ml) was added to a solution of 5-nitrosalicylaldehyde (334 mg, 2.0 mmol) in ethanol (10 ml). The mixture was stirred at $55\text{--}60\text{ }^\circ\text{C}$ for 6 h. After cooling to room temperature, the precipitate was filtered off and an orange red powder crystalline solid was obtained. Yield, 541 mg (68.8%). M.p. $117\text{--}118\text{ }^\circ\text{C}$. ^1H NMR (400 MHz, CDCl_3) δ

TABLE 1 Crystallographic data and refinement parameters for the complexes **1–4**

Complex	1	2	3	4
Empirical formula	C ₄₂ H ₅₀ Cl ₂ Ni ₃ N ₆ O ₂₀	C ₄₄ H ₅₂ Cl ₂ Ni ₃ N ₆ O ₁₉	C ₄₄ H ₄₈ Cl ₂ Ni ₃ N ₈ O ₁₈	C ₄₆ H ₅₈ Cl ₂ Ni ₃ N ₆ O ₂₀ S ₄
Formula weight	1205.91	1215.94	1223.93	1390.19
T (K)	296 (2)	150.00(10)	294 (2)	294.54(10)
Wavelength (Å)	0.71073	0.71073	0.71073	0.71073
Crystal system	triclinic	orthorhombic	triclinic	monoclinic
Space group	<i>P</i> -1	<i>P</i> 2 ₁ 2 ₁ 2 ₁	<i>P</i> -1	<i>P</i> 2 ₁ / <i>c</i>
<i>a</i> (Å)	10.922 (12))	20.6301 (14)	9.2381 (10)	13.5766 (13)
<i>b</i> (Å)	11.263 (12)	20.3857 (12)	12.816 (2)	16.0286 (15)
<i>c</i> (Å)	11.375 (12)	12.1769 (9)	13.749 (3)	15.7655 (13)
α (°)	84.896 (15)	90	69.663 (18)	90
β (°)	74.300 (16)	90	83.488 (13)	96.941 (8)
γ (°)	69.704 (16)	90	83.725 (11)	90
<i>V</i> (Å ³)	1263 (2)	5121.1 (6)	1512.2 (5)	3405.6 (5)
<i>Z</i>	1	4	1	2
<i>D</i> _{calc} (g·cm ⁻³)	1.585	1.577	1.344	1.356
μ (mm ⁻¹)	1.294	1.276	1.081	1.088
<i>F</i> (000)	622	2512	630	1436
Crystal size (mm)	0.18 × 0.15 × 0.11	0.13 × 0.11 × 0.04	0.31 × 0.26 × 0.25	0.31 × 0.25 × 0.24
θ Range (°)	1.86–27.71	3.402–26.022	3.40–26.013	3.304–25.680
Index ranges	-6 ≤ <i>h</i> ≤ 14 -14 ≤ <i>k</i> ≤ 14 -14 ≤ <i>l</i> ≤ 14	-15 ≤ <i>h</i> ≤ 25 -25 ≤ <i>k</i> ≤ 23 -8 ≤ <i>l</i> ≤ 1	-11 ≤ <i>h</i> ≤ 11 -14 ≤ <i>k</i> ≤ 15 -16 ≤ <i>l</i> ≤ 16	-16 ≤ <i>h</i> ≤ 16 -19 ≤ <i>k</i> ≤ 14 -19 ≤ <i>l</i> ≤ 19
Reflections collected	8336	15394	10420	19674
Unique reflections	5766	9615	5925	6283
<i>R</i> _{int}	0.0732	0.0750	0.0952	0.1439
Completeness to (%) (θ)	99.2 (25.24)	99.6 (26.00)	99.4 (25.24)	97.3 (25.24)
Data/restraints/ parameters	5766 / 44 / 354	9615 / 131 / 746	5925 / 64 / 380	6283 / 86 / 429
Goodness of fit (GOF)	0.921	0.970	0.968	0.975
Final <i>R</i> ₁ , <i>wR</i> ₂ indices	0.0723, 0.1729	0.0728, 0.0861	0.0801, 0.1493	0.0839, 0.1816
<i>R</i> ₁ , <i>wR</i> ₂ indices (all data)	0.1627, 0.2166	0.1483, 0.1179	0.1703, 0.2008	0.1769, 0.2485
Residuals peak / hole (e Å ⁻³)	1.078 and - 1.10	0.730 and - 0.519	0.763 and - 0.533	0.905 and - 0.609

**SCHEME 1** The synthetic route to H₂L

2.18 (t, *J* = 6.0 Hz, 2H, CH₂), 4.35 (m, 4H, CH₂), 6.91 (d, *J* = 4.0 Hz, 1H, ArH), 7.04 (d, *J* = 6.0 Hz, 1H, ArH), 7.13 (s, 1H, ArH), 7.23 (dd, *J* = 8 Hz, 1H, ArH), 8.14 (d,

J = 4.0 Hz, 1H, ArH), 8.16 (s, 1H, ArH), 8.19 (s, 1H, CH=N), 8.26 (s, 1H, CH=N), 9.77 (s, 1H, OH), 10.65 (s, 1H, OH). IR (KBr; cm⁻¹): 3084 [w, ν (O-H)], 1613 [s, ν (C=N)], 1263 [s, ν (Ar-O)]. UV-vis [EtOH], λ_{\max} (nm) [1.0 × 10⁻⁵ M] 219, 267 and 311. Anal. calc. For C₁₇H₁₆ClN₃O₆ (%): C, 51.77; H, 4.21; N, 10.59, Found (%): C, 51.95; H, 4.10; N, 10.37.

4.4 | Syntheses of the Ni(II) complexes **1–4**

Four solvent-induced the Ni(II) complexes **1–4** are obtained via the reaction of asymmetric Salamo-

type ligand H_2L with $Ni(OAc)_2 \cdot 4H_2O$ in a 2:3 molar ratio in absolute methanol, n-propanol, water, N,N-dimethylformamide and dimethyl sulphoxide solvents, respectively.

4.4.1 | Synthesis of the complex 1

A solution of $Ni(OAc)_2 \cdot 4H_2O$ (3.73 mg, 0.015 mmol) in methanol (3 ml) was added dropwise to a solution of H_2L (3.90 mg, 0.010 mmol) in acetone (1 ml). The color of the mixed solution changed to pale green immediately. After stirring for 10 min at room temperature, the mixture was filtered and the filtrate was allowed to stand at room temperature for about two weeks. Through partial solvent evaporation, several pale green block-shaped single crystals suitable for X-ray diffraction analysis were obtained after two weeks. Yield, 3.45 mg (57.2%). UV-vis [EtOH], λ_{max} (nm) [1.0×10^{-5} M]: 231, 376. IR (KBr; cm^{-1}): 1606 [s, $\nu(C=N)$], 1576 [s, $\nu_{as}(COO^-)$], 1425 [s, $\nu_s(COO^-)$], 1256 [w, $\nu(Ar-O)$]. Anal. calc. For $C_{42}H_{50}Cl_2N_6Ni_3O_{20}$ (%): C, 41.83; H, 4.18; N, 6.97; Ni, 14.60. Found (%): C, 41.68; H, 4.15; N, 7.03; Ni, 14.63.

4.4.2 | Synthesis of the complex 2

A solution of $Ni(OAc)_2 \cdot 4H_2O$ (3.75 mg, 0.015 mmol) in n-propanol (2 ml) was added dropwise to a mixture solution of acetone (1.0 ml) and water (0.5 ml) of H_2L (3.96 mg, 0.010 mmol). The color of the mixed solution changed to pale green immediately. After stirring for 15 min at room temperature, The mixture was filtered and the filtrate was allowed stand in the dark at room temperature for about two weeks, Through partial solvent evaporation, several pale green block-shaped single crystals suitable for X-ray diffraction analysis were obtained after two weeks. Yield, 3.09 mg (50.9%). UV-vis [EtOH], λ_{max} (nm) [1.0×10^{-5} M]: 232, 375. IR (KBr; cm^{-1}): 1652 [s, $\nu(C=O)$], 1608 [s, $\nu(C=N)$], 1557 [s, $\nu_{as}(COO^-)$], 1419 [s, $\nu_s(COO^-)$], 1253 [w, $\nu(Ar-O)$]. Anal. calc. For $C_{44}H_{52}Cl_2N_6Ni_3O_{19}$ (%): C, 43.46; H, 4.31; N, 6.91; Ni, 14.48. Found (%): C, 43.39; H, 4.27; N, 6.98; Ni, 14.56.

4.4.3 | Synthesis of the complex 3

A solution of $Ni(OAc)_2 \cdot 4H_2O$ (3.72 mg, 0.015 mmol) in methanol (2 ml) was added dropwise to a mixture solution of acetone (1 ml) and DMF (0.5 ml) of H_2L (3.91 mg, 0.010 mmol). The color of the mixed solution changed to pale green immediately. After stirring for 15 min at room temperature, the mixture was filtered and the filtrate was allowed to stand in the dark at room temperature for about two weeks, the solvent partially

evaporated and several pale green block-shaped single crystals suitable for X-ray crystallographic analysis were obtained. Yield, 2.86 mg (46.7%). UV-vis [EtOH], λ_{max} (nm) [1.0×10^{-5} M]: 230, 373. IR (KBr; cm^{-1}): 1652 [s, $\nu(C=O)$], 1606 [s, $\nu(C=N)$], 1577 [s, $\nu_{as}(COO^-)$], 1419 [s, $\nu_s(COO^-)$], 1250 [w, $\nu(Ar-O)$]. Anal. calc. For $C_{44}H_{48}Cl_2N_8Ni_3O_{18}$ (%): C, 43.18; H, 3.95; N, 9.16; Ni, 14.39. Found (%): C, 43.09; H, 3.90; N, 9.21; Ni, 14.53.

4.4.4 | Synthesis of the complex 4

A solution of $Ni(OAc)_2 \cdot 4H_2O$ (3.74 mg, 0.015 mmol) in methanol (2 ml) was added dropwise to a mixture solution of acetone (1.0 ml) and DMSO (0.5 ml) of H_2L (3.95 mg, 0.010 mmol). The color of the mixed solution changed to pale yellow immediately. After stirring for 10 min at room temperature, the mixture was filtered and the filtrate was allowed to stand in the dark at room temperature for about two weeks, the solvent partially evaporated and several pale yellow block-shaped single crystals suitable for X-ray crystallographic analysis were obtained. Yield, 3.03 mg (43.5%). UV-vis [EtOH], λ_{max} (nm) [1.0×10^{-5} M]: 231, 371. (1.0×10^{-5} M). IR (KBr; cm^{-1}): 1613 [s, $\nu(C=N)$], 1576 [s, $\nu_{as}(COO^-)$], 1425 [s, $\nu_s(COO^-)$], 1250 [w, $\nu(Ar-O)$]. Anal. calc. for $C_{46}H_{58}Cl_2N_6Ni_3O_{20}S_4$ (%): C, 39.74; H, 4.21; N, 6.05; Ni, 12.67. Found (%): C, 39.69; H, 4.09; N, 5.92; Ni, 12.73.

ACKNOWLEDGEMENTS

This work was supported by the National Natural Science Foundation of China (21761018) and the Program for Excellent Team of Scientific Research in Lanzhou Jiaotong University (201706), which is gratefully acknowledged.

ORCID

Wen-Kui Dong  <http://orcid.org/0000-0003-1249-5808>

REFERENCES

- [1] J. Costamagna, J. Vargas, R. Latorre, A. Alvarado, G. Mena, *Coor. Chem. Rev.* **1992**, 119, 67.
- [2] Y. X. Sun, L. Xu, T. H. Zhao, S. H. Liu, G. H. Liu, X. T. Dong, *Synth. React. Inorg. Met.-Org. Nano-Met. Chem.* **2013**, 43, 509.
- [3] X. Q. Song, Y. Q. Peng, G. Q. Chen, X. R. Wang, P. P. Liu, *Inorg. Chim. Acta* **2015**, 427, 13.
- [4] X. Q. Song, P. P. Liu, Z. R. Xiao, X. Li, Y. A. Liu, *Inorg. Chim. Acta* **2015**, 438, 232.
- [5] Y. X. Sun, X. H. Gao, *Synth. React. Inorg. Met.-Org. Nano-Met. Chem.* **2011**, 41, 973.

- [6] D. J. Darensbourg, *Chem. Rev.* **2007**, *107*, 2388.
- [7] X. Y. Dong, X. Y. Li, L. Z. Liu, H. Zhang, Y. J. Ding, W. K. Dong, *RSC Adv.* **2017**, *7*, 48394.
- [8] H. L. Wu, G. L. Pan, Y. C. Bai, H. Wang, J. Kong, F. R. Shi, Y. H. Zhang, X. L. Wang, *J. Chem. Res.* **2014**, *38*, 211.
- [9] H. L. Wu, G. L. Pan, Y. C. Bai, H. Wang, J. Kong, F. R. Shi, Y. H. Zhang, X. L. Wang, *J. Coord. Chem.* **2013**, *66*, 2634.
- [10] H. L. Wu, Y. C. Bai, Y. H. Zhang, G. L. Pan, J. Kong, F. R. Shi, X. L. Wang, *Z. Anorg. Allg. Chem.* **2014**, *640*, 2062.
- [11] C. Y. Chen, J. W. Zhang, Y. H. Zhang, Z. H. Yang, H. L. Wu, G. L. Pan, Y. C. Bai, *J. Coord. Chem.* **2015**, *68*, 1054.
- [12] H. L. Wu, C. P. Wang, F. Wang, H. P. Peng, H. Zhang, Y. C. Bai, *J. Chinese Chem. Soc.* **2015**, *62*, 1028.
- [13] H. L. Wu, G. L. Pan, Y. C. Bai, H. Wang, J. Kong, F. R. Shi, Y. H. Zhang, X. L. Wang, *Res. Chem. Intermed.* **2015**, *41*, 3375.
- [14] H. L. Wu, Y. C. Bai, Y. H. Zhang, Z. Li, M. C. Wu, C. Y. Chen, J. W. Zhang, *J. Coord. Chem.* **2014**, *67*, 3054.
- [15] C. D. Ene, S. Nastase, C. Maxim, A. M. Madalan, F. Tuna, M. Andruh, *Inorg. Chim. Acta* **2010**, *363*, 4247.
- [16] P. P. Liu, L. Sheng, X. Q. Song, W. Y. Xu, Y. A. Liu, *Inorg. Chim. Acta* **2015**, *434*, 252.
- [17] X. Q. Song, P. P. Liu, Y. A. Liu, J. J. Zhou, X. L. Wang, *Dalton Trans.* **2016**, *45*, 8154.
- [18] L. Q. Chai, K. Y. Zhang, L. J. Tang, J. Y. Zhang, H. S. Zhang, *Polyhedron* **2017**, *130*, 100.
- [19] W. K. Dong, J. C. Ma, L. C. Zhu, Y. Zhang, *New J. Chem.* **2016**, *40*, 6998.
- [20] Y. X. Sun, S. T. Zhang, Z. L. Ren, X. Y. Dong, *Synth. React. Inorg. Met.-Org. Nano-Met. Chem.* **2013**, *43*, 995.
- [21] L. Chen, W. K. Dong, H. Zhang, Y. Zhang, Y. X. Sun, *Cryst. Growth Des.* **2017**, *17*, 3636.
- [22] Y. X. Sun, L. Wang, X. Y. Dong, Z. L. Ren, W. S. Meng, *Synth. React. Inorg. Met.-Org. Nano-Met. Chem.* **2013**, *43*, 599.
- [23] L. Q. Chai, G. Wang, Y. X. Sun, W. K. Dong, L. Zhao, X. H. Gao, *J. Coord. Chem.* **2012**, *65*, 1621.
- [24] W. K. Dong, X. L. Li, L. Wang, Y. Zhang, Y. J. Ding, *Sens. Actuators B* **2016**, *229*, 370.
- [25] W. K. Dong, S. F. Akogun, Y. Zhang, Y. X. Sun, X. Y. Dong, *Sens. Actuators B* **2017**, *238*, 723.
- [26] B. J. Wang, W. K. Dong, Y. Zhang, S. F. Akogun, *Sens. Actuators B* **2017**, *247*, 254.
- [27] F. Wang, L. Gao, Q. Zhao, Y. Zhang, W. K. Dong, Y. J. Ding, *Spectrochim. Acta. A* **2018**, *190*, 111.
- [28] L. Q. Chai, G. Liu, J. Y. Zhang, J. J. Huang, J. F. Tong, *J. Coord. Chem.* **2013**, *66*, 3926.
- [29] X. Y. Dong, Q. P. Kang, B. X. Jin, W. K. Dong, *Z. Naturforsch.* **2017**, *72*, 415.
- [30] P. P. Liu, C. Y. Wang, M. Zhang, X. Q. Song, *Polyhedron* **2017**, *129*, 133.
- [31] X. Q. Song, Q. F. Zheng, L. Wang, W. S. Liu, *Luminescence* **2012**, *27*, 459.
- [32] W. K. Dong, J. C. Ma, L. C. Zhu, Y. X. Sun, S. F. Akogun, Y. Zhang, *Cryst. Growth Des.* **2016**, *16*, 6903.
- [33] X. Y. Dong, Y. X. Sun, L. Wang, L. Li, *J. Chem. Res.* **2012**, *36*, 387.
- [34] L. Zhao, L. Wang, Y. X. Sun, W. K. Dong, X. L. Tang, X. H. Gao, *Synth. React. Inorg. Met. Org. Nano Met. Chem.* **2012**, *42*, 1303.
- [35] L. Zhao, X. T. Dang, Q. Chen, J. X. Zhao, L. Wang, *Synth. React. Inorg. Met. Org. Nano Met. Chem.* **2013**, *43*, 1241.
- [36] P. Wang, L. Zhao, *Spectrochim. Acta, Part A* **2015**, *135*, 342.
- [37] V. T. Kasumov, F. Köksal, *Spectrochim. Acta, Part A* **2005**, *61*, 225.
- [38] S. Akine, T. Taniguchi, W. K. Dong, S. Masubuchi, T. Nabeshima, *J. Org. Chem.* **2005**, *70*, 1704.
- [39] L. Gao, F. Wang, Q. Zhao, Y. Zhang, W. K. Dong, *Polyhedron* **2018**, *139*, 7.
- [40] P. Wang, L. Zhao, *Synth. React. Inorg. Met.-Org Nano-Met. Chem.* **2016**, *46*, 1095.
- [41] L. Wang, J. Hao, L. X. Zhai, Y. Zhang, W. K. Dong, *Crystals* **2017**, *7*, 277.
- [42] L. Wang, J. C. Ma, W. K. Dong, L. C. Zhu, Y. Zhang, *Z. Anorg. Allg. Chem.* **2016**, *642*, 834.
- [43] W. K. Dong, Y. X. Sun, C. Y. Zhao, X. Y. Dong, L. Xu, *Polyhedron* **2010**, *29*, 2087.
- [44] M. Asadi, K. A. Jamshid, A. H. Kyanfar, *Inorg. Chim. Acta* **2007**, *360*, 1725.
- [45] A. Majumder, G. M. Rosair, A. Mallick, N. Chattopadhyay, S. Mitra, *Polyhedron* **2006**, *25*, 1753.
- [46] L. Wang, X. Y. Li, Q. Zhao, L. H. Li, W. K. Dong, *RSC Adv.* **2017**, *7*, 48730.
- [47] L. Xu, L. C. Zhu, J. C. Ma, Y. Zhang, J. Zhang, W. K. Dong, *Z. Anorg. Allg. Chem.* **2015**, *641*, 2520.
- [48] X. Y. Li, L. Chen, L. Gao, Y. Zhang, S. F. Akogun, W. K. Dong, *RSC Adv.* **2017**, *7*, 35905.
- [49] L. Q. Chai, L. J. Tang, L. C. Chen, J. J. Huang, *Polyhedron* **2017**, *122*, 228.
- [50] W. Y. Bi, X. Q. Lv, W. L. Chai, W. J. Jin, J. R. Song, W. K. Dong, *Inorg. Chem. Commun.* **2008**, *11*, 1316.
- [51] W. K. Dong, J. T. Zhang, Y. J. Dong, Y. Zhang, Z. K. Wang, *Z. Anorg. Allg. Chem.* **2016**, *642*, 1896.
- [52] W. K. Dong, J. Zhang, Y. Zhang, N. Li, *Inorg. Chim. Acta* **2016**, *444*, 95.
- [53] C. H. Tao, J. C. Ma, L. C. Zhu, Y. Zhang, W. K. Dong, *Polyhedron* **2017**, *128*, 38.
- [54] G. Li, J. Hao, L. Z. Liu, W. M. Zhou, W. K. Dong, *Crystals* **2017**, *7*, 217.
- [55] X. Q. Song, G. Q. Cheng, X. R. Wang, W. Y. Xu, P. P. Liu, *Inorg. Chim. Acta* **2015**, *425*, 145.
- [56] Y. J. Dong, J. C. Ma, L. C. Zhu, W. K. Dong, Y. Zhang, *J. Coord. Chem.* **2017**, *70*, 103.
- [57] X. Y. Li, Q. P. Kang, L. Z. Liu, J. C. Ma, W. K. Dong, *Crystals* **2018**, *8*, 43.
- [58] S. Akine, A. Akimoto, T. Shiga, H. Oshio, T. Nabeshima, *Inorg. Chem.* **2008**, *47*, 875.

- [59] W. K. Dong, L. C. Zhu, Y. J. Dong, J. C. Ma, Y. Zhang, *Polyhedron* **2016**, *117*, 148.
- [60] L. Gao, C. Liu, F. Wang, W. K. Dong, *Crystals* **2018**, *8*, 77.
- [61] J. C. Ma, X. Y. Dong, W. K. Dong, Y. Zhang, L. C. Zhu, J. T. Zhang, *J. Coord. Chem.* **2016**, *69*, 149.
- [62] G. M. Sheldrick and SHELXS-97, Program for the Solution of Crystal Structures; University of Göttingen, Göttingen Germany, **1997**.
- [63] G. M. Sheldrick and SHELXL-97, Program for the Refinement of Crystal Structures; University of Göttingen, Göttingen Germany, **1997**.
- [64] S. Akine, T. Taniguchi, T. Nabeshima, *Chem. Lett.* **2001**, *30*, 682.
- [65] S. Akine, W. K. Dong, T. Nabeshima, *Inorg. Chem.* **2006**, *45*, 4677.

SUPPORTING INFORMATION

Additional Supporting Information may be found online in the supporting information tab for this article.

CCDC 1814381–1814384 contains the supplementary crystallographic data for the complexes **1–4**. These data can be obtained free of charge via <http://www.ccdc.cam.ac.uk/conts/retrieving.html>, or from the Cambridge Crystallographic Data Centre, 12 Union Road, Cambridge CB2 1EZ, UK; fax: (+44) 1223–336–033; or e-mail: deposit@ccdc.cam.ac.uk.

How to cite this article: Kang Q-P, Li X-Y, Zhao Q, Ma J-C, Dong W-K. Structurally characterized homotrinary Salamo-type nickel(II) complexes: Synthesis, solvent effect and fluorescence properties. *Appl Organometal Chem.* 2018;e4379. <https://doi.org/10.1002/aoc.4379>